Journal of Power Sources 190 (2009) 56–63

Contents lists available at ScienceDirect

Journal of Power Sources

journal homepage: www.elsevier.com/locate/jpowsour

Nonlinear empirical model of gas humidity-related voltage dynamics of a polymer-electrolyte-membrane fuel cell stack

M. Meiler[a,*], D. Andre[a], O. Schmid[a], E.P. Hofer[b]

[a] Department of MEA and Stack Technology, Daimler AG, Neue Str. 95, D-73230 Kirchheim/Teck, Germany
[b] Institute of Measurement, Control and Microtechnology, University of Ulm, Albert-Einstein-Allee 41, D-89081 Ulm, Germany

ARTICLE INFO

Article history:
Received 10 June 2008
Received in revised form 7 August 2008
Accepted 8 August 2008
Available online 22 August 2008

Keywords:
Polymer-electrolyte-membrane fuel cell
Dynamic model
Gas humidity
System identification

ABSTRACT

Intelligent energy management is a cost-effective key path to realize efficient automotive drive trains [R. O'Hayre, S.W. Cha, W. Colella, F.B. Prinz. Fuel Cell Fundamentals, John Wiley & Sons, Hoboken, 2006]. To develop operating strategy in fuel cell drive trains, precise and computational efficient models of all system components, especially the fuel cell stack, are needed. Should these models further be used in diagnostic or control applications, then some major requirements must be fulfilled. First, the model must predict the mean fuel cell voltage very precisely in all possible operating conditions, even during transients. The model output should be as smooth as possible to support best efficient optimization strategies of the complete system. At least, the model must be computational efficient. For most applications, a difference between real fuel cell voltage and model output of less than 10 mV and 1000 calculations per second will be sufficient. In general, empirical models based on system identification offer a better accuracy and consume less calculation resources than detailed models derived from theoretical considerations [J. Larminie, A. Dicks. Fuel Cell Systems Explained, John Wiley & Sons, West Sussex, 2003]. In this contribution, the dynamic behaviour of the mean cell voltage of a polymer-electrolyte-membrane fuel cell (PEMFC) stack due to variations in humidity of cell's reactant gases is investigated. The validity of the overall model structure, a so-called general Hammerstein model (or Uryson model), was introduced recently in [M. Meiler, O. Schmid, M. Schudy, E.P. Hofer. Dynamic fuel cell stack model for real-time simulation based on system identification, J. Power Sources 176 (2007) 523–528]. Fuel cell mean voltage is calculated as the sum of a stationary and a dynamic voltage component. The stationary component of cell voltage is represented by a lookup-table and the dynamic voltage by a parallel placed, nonlinear transfer function. A suitable experimental setup to apply fast variations of gas humidity is introduced and is used to investigate a 10 cell PEMFC stack under various operation conditions. Using methods like stepwise multiple-regression a good mathematical description with reduced free parameters is achieved.

1. Introduction

Fuel cell vehicles are a promising alternative to vehicles powered by internal combustion engines because of their low noise and zero-emission. The core piece of a fuel cell power train is a stack of polymer-electrolyte-membrane fuel cells (PEMFCs) supplied with hydrogen and oxygen.

One of the major issues in the operation of PEMFC stacks is a satisfying humidification, since the humidification level of the stack plays a decisive role for performance. First of all, the proton conductivity of the membrane is proportional to the water content [1]. The membrane is a derivation of polytetrafluoroethylene (PTFE) with an additional compound of H^+–SO_3^-. In the presence of water, this bond is just weak and channels for motile protons will be created [2]. The protons drag water molecules from anode to cathode by an electro-osmotic effect and in consequence, the anode contains less water than the cathode, where furthermore water is produced. However, also the cathode will dry out at high temperatures or high flow rates. To avoid this drying, to balance the different humidification levels of the electrodes, and to minimize the overvoltage caused by membrane resistance, the gas must be humidified before entering the stack. But even an excess of humidification can decrease the stack performance if water floods the electrodes, blocks the pores in the gas diffusion layer, and so decrease the mass transport significantly. Therefore, a controlled water balance is an important task for the operation of a PEMFC stack.

* Corresponding author. Tel.: +49 7021 89 35 20; fax: +49 711 30 52 19 35 20.
E-mail address: markus.meiler@daimler.com (M. Meiler).

0378-7753/$ – see front matter © 2008 Elsevier B.V. All rights reserved.
doi:10.1016/j.jpowsour.2008.08.029

In transportation applications, the stack voltage is dependent of several surrounding conditions and 80% of operating situations are dynamic [3]. The development of new operating strategies is therefore a challenging task. In particular the influence of fuel cell gas humidity, a high relation to dynamic behaviour of stack voltage can be found.

So far, only models for the static behaviour of stack voltage in relation to gas flow humidity are known in literature [4,5]. In this work, a valid model for the simulation of the dynamic behaviour of stack voltage by variation of fuel cell gas humidity is introduced and developed for the first time. The aim of this work is to provide a simulation tool which:

- simulates the stack voltage with a precise prediction,
- is valid in power train relevant operating area,
- uses an easy and reliable identification,
- is suitable for simulations in real-time.

2. Theoretical background

2.1. Gas humidification

The saturation pressure E of steam can be approximated with the actual steam inlet temperature T (in °C) by using the Magnus equation for water [6] as given in the following equation:

$$E = 610.78\,\text{Pa} \times 10^{(7.5T/(237.3+T))} \tag{1}$$

Using this saturation pressure, the steam pressure e as function of the desired relative humidity rh can be calculated using the following equation:

$$e = \text{rh}\,E \tag{2}$$

The mixing ratio mr is defined by the ratio of mass flow of steam $\dot{m}_{H_2O}$ to mass flow of dry gas $\dot{m}_{gas,dry}$ or with the molar masses $M_{gas,dry}$, M_{H_2O}, and the absolute pressure of the gas p, respectively:

$$\text{mr} = \frac{\dot{m}_{H_2O}}{\dot{m}_{gas,dry}} = \frac{M_{H_2O}}{M_{gas,dry}}\frac{e}{p-e} \tag{3}$$

Thus, the required steam mass flow can be calculated by the following equation:

$$\dot{m}_{H_2O} = \text{mr}\,\dot{m}_{gas,dry} \tag{4}$$

2.2. Stepwise regression analysis

A structured process to determine an empirical model is the stepwise regression method [7]. The aim of this method is to gain a linear model equation for the target variable, which is as simple as possible but still estimates the output variable with a high accuracy [8]. Stepwise regression analysis is a well-known process in statistical analysis of experimental data [7]. A short overview on the method is given in the next paragraphs. For more detailed background information we refer to Refs. [7–11].

First of all, a linear model is taken with terms of all input variables, transformation of these ones (mostly squared, logarithmic, exponential, and reciprocal), and interactions between the input variables. After the parameter estimation, a null hypothesis is tested for each estimated parameter ξ, as described in Refs. [10,12,13]. The null hypothesis is denied if the probability of the test Ψ is smaller than the chosen significance level Ψ_{out} and therefore, the tested coefficient ξ remains in the model. If the probability is greater than the significance level ($\Psi > \Psi_{out}$) the tested coefficient is assumed to be zero and the corresponding term is taken out of the model. To improve numerical stability and to speed up regression convergence, a second, smaller significance level Ψ_{in} can be defined. If the probability of the null hypothesis Ψ is smaller than entrance level Ψ_{in} ($\Psi < \Psi_{in}$) the null hypothesis has to be rejected and the tested term is included into the model. As result, a reduced linear model with only the most significant parameters is available to predict the output variable. If there are more model terms ϕ than experimental data Φ available, not included terms are added to model individually and their Ψ-values are calculated successively. The term with the smallest Ψ-values is added to the model. This is repeated until no excluded terms have a Ψ-values below Ψ_{out}.

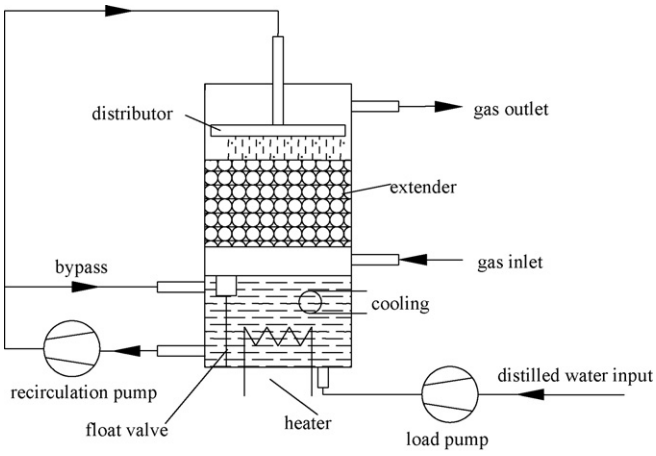

Fig. 1. Flow diagram of humidification by bubbler-humidifier.

Following, the used equations during stepwise regression are described briefly. First, the optimal parameters ξ of the linear model:

$$\hat{Y} = X\xi \tag{5}$$

have to be estimated. X is a Φ-by-ϕ matrix of the input variables and $\hat{Y}$ the vector of the estimated output variable K_D. The estimation of the model quality is possible by the square error amount J between the estimated and measured output variable:

$$J = \sum_{d=1}^{\Phi}(Y_d - \hat{Y}_d)^2 = \sum_{d=1}^{\Phi}(Y_d - X_d\xi)^2 \tag{6}$$

Since the parameters for the minimum J have to be found, Eq. (6) has to be minimized by differentiation and must be zero. Finally, the optimal parameters can be calculated by the following equation:

$$\xi = (X'X)^{-1}X'Y \tag{7}$$

The next step is to determine the standard deviation s_θ for each parameter (with parameter index $\theta = 1\ldots\phi$), which is defined by the product of the standard deviation of the regression $s_{regression}$ and the variance of each variable, which can be found in the main diagonal elements of the covariance matrix as described in the following equation:

$$s_\theta = s_{regression}\sqrt{((X'X)^{-1})_{\theta\theta}} \tag{8}$$

For the calculation of $s_{regression}$ (Eq. (9)), is the degree of freedom ϑ defined by the difference between the number of experimental Φ data and the number of parameters ϕ, is important:

$$s_{regression} = \sqrt{\frac{\sum_{d=1}^{\Phi}(Y_d - \hat{Y}_d)^2}{\vartheta}} \tag{9}$$

The ratio of parameter and standard deviation is the Student-factor t of the null hypothesis test:

$$t_\theta = \frac{b_\theta}{s_\theta} \tag{10}$$

By knowing this value, the probability Ψ can be calculated by solving the integral of the t-distribution function:

$$\Psi_\theta = 2\int_{t_\theta}^{\infty} \frac{\Gamma((\vartheta+1)/2)}{\sqrt{\vartheta\pi}\,\Gamma(\vartheta/2)}\left(1+\frac{x^2}{\vartheta}\right)^{\vartheta+1/2} \mathrm{d}x \tag{11}$$

with Γ the gamma function (Eq. (12)):

$$\Gamma(f) = \int_0^{\infty} e^{-s}s^{f-1}\,ds \tag{12}$$

Thus, it is possible to calculate Ψ_θ for every variable of the polynomial. To evaluate the quality of the resulting model, a good criterion is the degrees of freedom adjusted R-square (R^2_{adj}). Therefore, the sum of squares due to error (SSE) has to be calculated as given in the following equation:

$$\mathrm{SSE} = \sum_{d=1}^{\Phi}(Y_d - \hat{Y}_d)^2 \tag{13}$$

With the mean value $\bar{Y}_d$ the sum of squares about the mean (SSM) can be calculated:

$$\mathrm{SSM} = \sum_{d=1}^{\Phi}(Y_d - \bar{Y}_d)^2 \tag{14}$$

Then, a measure for model quality is developed, the so-called R-square (R^2):

$$R^2 = 1 - \frac{\mathrm{SSE}}{\mathrm{SSM}} \tag{15}$$

The disadvantage of this measure is that it always becomes larger while adding more parameters to the model. This problem can be solved by introducing the degrees of freedom adjusted R-square (R^2_{adj}) [10]:

$$R^2_{\mathrm{adj}} = 1 - \frac{\mathrm{SSE}(\Phi-1)}{\mathrm{SSM}(\vartheta)} \tag{16}$$

The R^2_{adj} declines if additional model parameters do not significantly decrease SSE.

3. Experimental work

3.1. Direct steam injection (DSI)

Our team showed recently [3] that the investigation of dynamic behaviour by step response and identification of the corresponding transfer function is a promising way.

For dynamic analysis, the investigated system has to be able to manage step responses fast and without a delay. This assumption is not achieved by state of the art in humidification, the so-called bubbler-humidifiers. A typical bubbler-humidifier and the corresponding working-principle are depicted in Fig. 1.

On its way to the stack, the gas has to pass a packed bed and absorbs thereby down streaming water. The variable of interest, the relative humidity rh, can be controlled by adjusting the ratio of temperature in the humidifier and temperature in the stack. Since the gas leaves the humidifier with the dew point temperature, the gas will always have a relative humidity of rh = 1.00 when it is entering the stack. Because of its low heat capacity, the gas will be matching to the stack temperature very fast in a heat exchanger and the relative humidity will change. If both temperatures have the same value, the relative humidity of 1.00 will be persist, however if the temperature of the gas is cooled down in the heat exchanger for example, from 75 to 59 °C, the relative humidity will just decrease to rh = 0.50.

The disadvantage of this robust and long-stable system is, as mentioned above, the missing ability to respond to variations in humidification fast enough because of its high inert thermal behaviour and its large volume. In order to identify transfer functions from experimental data, a system must be able to apply ideal steps with maximum time delays in the range of a few seconds. A bubbler-humidifier takes for the mentioned step in humidity about 4 min and is therefore inapplicable for dynamic investigations.

The problem is solved by the development of a more sophisticated system, enabling the direct injection of steam (DSI) instead of the time-intensive accumulation of water in a gas. A draft of the experimental set-up used for all tests can be found in Fig. 2.

The principle of DSI is the connection of a steam generator at the gas supply and the controlling of the entering steam amount by a mass flow controller (FIC 1 in Fig. 2), which will be explained later, in front of the mixing point between steam and dry gas. Heating tapes keep the temperature constant and so no water can condense till the temperature of the wet gas is matched with the stack temperature in a heat exchanger. The required amount of steam is calculated by the test bench software in real-time using Eqs. (1)–(4).

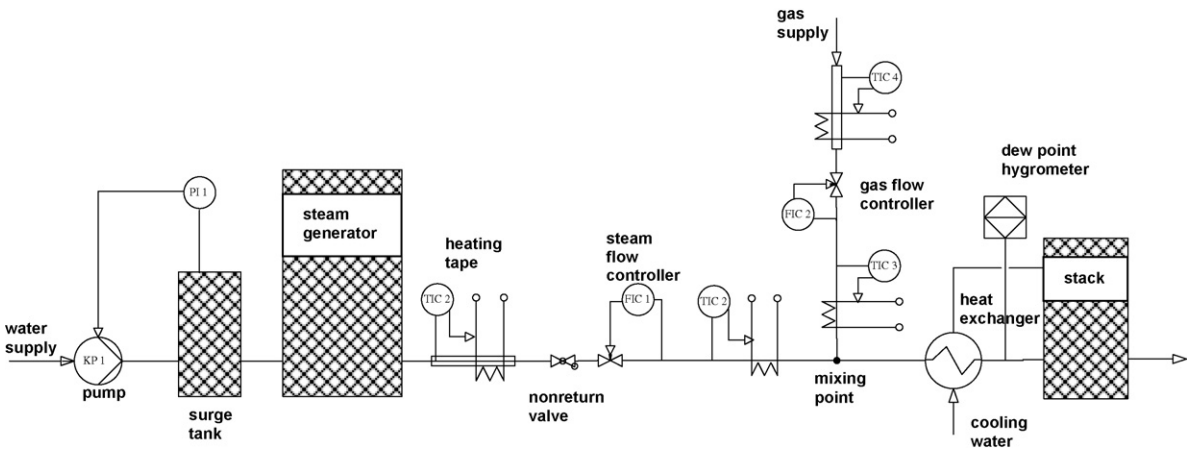

Fig. 2. Flow diagram of humidification by DSI.

As shown, it is possible to calculate the required steam amount only by measuring the mass flow of dry gas in front of the mixing point (FIC 2 in Fig. 2), the pressure of the gas at stack inlet, and the temperature (TIC 2 in Fig. 2) at stack inlet. For temperature measurement, coolant temperature is more suitable than gas temperature. The thermal energy of the coolant is 2 orders of magnitude higher than the thermal energy of the reactants. Due to a large available heat transfer area and the good thermal conductivity of the used materials, the gas temperature is rapidly adjusted to coolant temperature at the stack inlet.

Thermocouples and pressure sensors are cost-effective and accurate measuring sensors and were therefore chosen. Measurements of the mass flow are more complex and were realized by coriolis mass flow controller (CMFC) CORI-Flow from Bronkhorst. These sensors measure the created phase shifting of two oscillating curved tubes by coriolis force. When a mass flow is passing the tubes, CMFCs have great advantages like: real-time measurement, independence of material properties like density or viscosity and a high accuracy with a error of just about 0.2%. A more detailed description of the coriolis measuring principle is given in Ref. [14]. For the validation of the proposed humidification by direct steam injection precise measurement of gas humidity is necessary. Therefore, two common used capacitive hygrometers HTS 32D from Rotronic with a specified accuracy of 2% in relative humidity and a chilled mirror dew point hygrometer (CMDPH) DP3-D from MBW with an accuracy of less than 0.1% relative humidity are used.

CMDPHs are using the principle of cooling down a mirror thermoelectrically by a peltier device until the mirror reaches the dew point of the surrounding gas. At this temperature, the water will begin to form condensate on the mirror resulting in an improved absorption of emitting light. The decreased light reflection is noticing by a detector and a software is able to calculate the relative humidify using Eqs. (1) and (2). The used CMDPH is accurately calibrated by the manufacturer and is used as a reference during validation of the DSI method.

3.2. Cathode humidity cycling

All fuel cell tests were done on a test bench of Daimler using a PEMFC stack with metallic bipolar plates and commercial Membrane-Electrode-Assembly (MEAs). The stack design was developed by Daimler and was already used in previous work [3], because of its strong similarity to stacks used in Daimler's prototype fuel cell car F 600.

The stack consisted of ten cells, with an active area of 300 cm^2 each and is integrated under a pressure of 3 bar. All experiments are carried out in a fully software controlled Daimler's Fuel-Cell-Stack-Test-Bench. The cells are operated with cleaned air as cathode gas and a hydrogen/nitrogen mixture as anode gas. All gas flows are controlled by two mass flow controllers, one for small mass flows and one for large mass flows, to ensure a high accuracy in the whole operating area. The pressures of both gases are adjusted by digital controlled valves at the outlet and the stack temperature is controlled by varying the mass flow of cooling water.

The test bench allows measurements in the major operating area of fuel cell powered drive trains, in detail this are: a gauge pressure p until 2.6 bar, a stoichiometry λ (ratio of supplied reactant to chemically needed reactant) from 1.4 to 3, a current density i in the range of 0.4–1.6 A cm^{-2}, a stack inlet temperature T_{in} between 40 and 80 °C, and a difference between inlet and outlet temperature ΔT of 0–10 K. Restrictions had just been made in regard to comply with a maximum pressure difference of 500 mbar between anode and cathode. A further input parameter in all experiments is the fraction of H_2 in the anode gas c_{H_2}, since the diffusion of air from cathode to anode is a typical phenomenon of PEMFCs. In automotive drive trains this accumulation of N_2 is intensified by the recycling of anode gas by a H_2-loop and the fraction of hydrogen in the anode c_{H_2} is therefore a point of interest. In Table 1, the experimentally investigated operation conditions are summarized.

Table 1
Experimentally investigated conditions

Input Θ		Unit	Range
Current density	i	A cm^{-2}	0.4–1.6
Cathode gas stoichiometry	λ_c	–	1.4–3
Anode gas stoichiometry	λ_a	–	1.4–3
Cathode gas pressure	p_c	bar_a	1–2.6
Anode gas pressure	p_a	bar_a	1–2.6
Relative humidity anode gas	rh_a	–	0.33–1
Inlet temperature	T_{in}	°C	40–75
Outlet–inlet temperature	ΔT	°C	0–18
Hydrogen concentration	c_{H_2}	–	0.4–1

For covering the listed drive train relevant operating area reasonably, 101 operating conditions are investigated without applying harmful conditions to the stack.

A three level humidity cycle (rh_c = 0.33, 0.67, and 1.00) is conducted as described in Fig. 3 to stimulate cathode gas relative humidity-related voltage dynamics. With a sample rate of 1 Hz, the data are recorded, exported to MATLAB, and analysed in the next chapter.

4. Experimental results

4.1. DSI verification

The sensors for the measurements of relative humidity work like expected very slowly, about 1 h must be scheduled for getting an exact value. Therefore, the direct measurement of gas humidity is not possible. In Fig. 4, the measured relative humidity is plotted against the mass flow of steam injected into dry air for an air flow of 100 Nl min^{-1}. Furthermore, the calculated relative humidity (Eqs. (1)–(4)) using the measured steam mass flow, air mass flow, temperature, and pressure is given in Fig. 4.

The capacitive sensors are only used for having a comparison and, are because of a high average deviation of about 5% relative humidity and a maximum deviation of 30% points, are not sufficient for precise measurements and thus not used for calibration, whereas the CMDPH had only an average deviation of 0.5% and the deviations are low in the whole measuring range. For demonstrating the high accuracy of the DSI method in a large operating area, the CMDPH was tested also for smaller mass flows and the results are plotted in Fig. 5. The lines in the upper part of this figure show the experimental and calculated data for a mass flow of

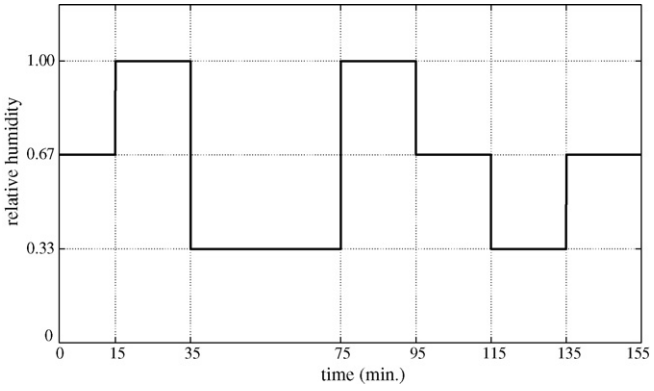

Fig. 3. Realized steps in humidity for every run.

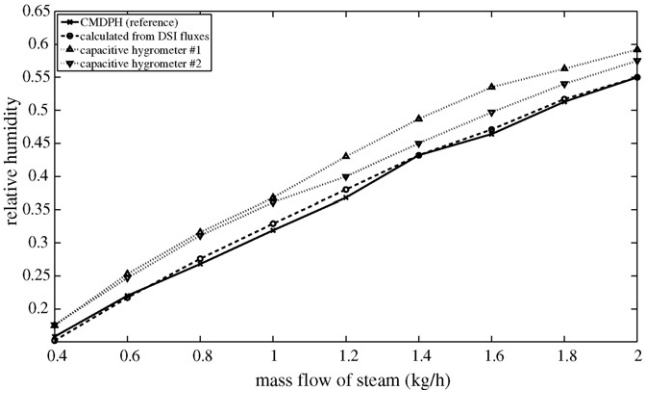

Fig. 4. Comparison of measured and calculated relative humidity for a mass flow of 100 Nl min^{-1} dry air.

20 Nl min^{-1} of dry air and the ones in the lower part for a mass flow of 50 Nl min^{-1} of dry air. The average deviations are again just low and as a consequence the CMDPH was used for the calibration before every measurement.

A very accurate and most of all, very dynamic method for varying the gas humidity is available now. Impressive proved by a time duration of just 2 s to manage the step from 0.50 to 1.00 in relative humidity and thus a strong enhancement to previous methods. Ref. [9] calls a system suitable for dynamic investigations if it is 2–10 times faster than the step response. In our case, the voltage needs at least 30 s or 15 times of the time of the system, so this rule of thumb is fulfilled and dynamic analysis is possible.

4.2. Cell voltage response

Similar to Ref. [15], the experimental data of the stack performance shows the effect that the water content of the membrane is more related to the cathode humidification than to the anode humidification. That means nearly no stationary voltage effect of anode humidification is observable even at low cathode gas humidification. Besides, no dynamic voltage can be seen for steps in the anode humidity and for this reason, just the cathode is investigated in the further work.

In different operation points (exemplary in figure caption Figs. 6 and 7) of the PEMFC system measurements were accomplished with the same cathode humidity cycle (Fig. 3). Afterwards the dynamic in the mean voltage is analysed according to cathode humidity.

Therefore, a correct predicting model had to be able to consider not only the static behaviour, but also the dynamic behaviour of the stack voltage in dependence on operating parameters.

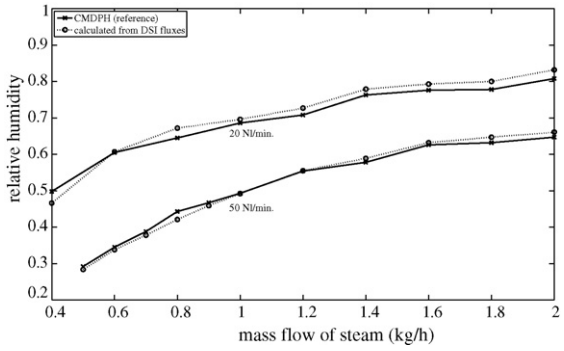

Fig. 5. Measured and calculated relative humidify for 20 and 50 Nl min^{-1} flow of dry air.

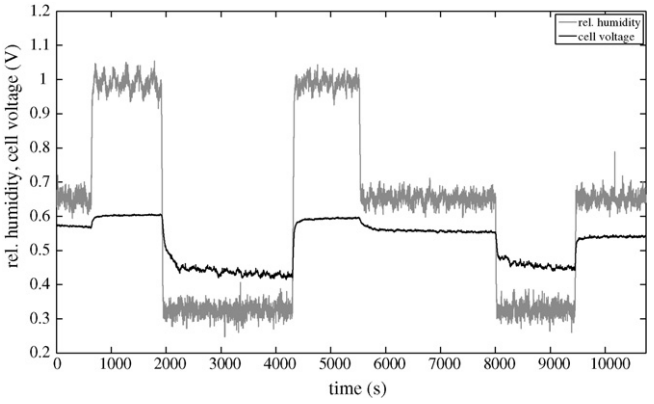

Fig. 6. Variation of humidity and measured step response of voltage in case of an operating point with strong dynamic (i = 1.4 A cm^{-2}, λ_c = 1.9, λ_a = 1.8, p_c = 1.8 bar, p_a = 2.2 bar, rh$_a$ = 0.33, T = 55 °C, ΔT = 10 K, c_{H_2} = 1).

One of the most interesting results of the experimental data analysis is the fact that two completely different behaviours of the system are observed when the cathode humidification is varied. In Fig. 6, the mean voltage of the ten cells shows a strong correlation to the humidity of the cathode, however, in Fig. 7, nearly no influence of the relative humidity is observable. Also important is the fact that the voltage in Fig. 6 shows a significant dynamic behaviour after each step. Fig. 6 shows that the cathode humidity of this operation point has a significant influence in the static and dynamic behaviour of the mean voltage. However, Fig. 7 shows an operation point with almost no influence of humidity in cell voltage. In dependence of the step height, it took 5–33 min till the new steady state is reached. In other publications the same behaviour of the cathode humidity according to the different amplitude of the mean cell voltage in different operation points can be observed [16–18].

5. Modelling of dynamic stack voltage

The total of 606 steps are divided into a set of 174 steps for parameter identification and the remaining ones for the independent validation of the gained model. For every of these 174 steps, the time constants were identified by an optimization function using the least square method.

The focus in this work is set on the modelling of the dynamic portion of cell voltage. This procedure saves the already done modelling of the static behaviour and allows the fusion of both portions at the end. The dynamic voltage U_{dynamic}, defined as the difference between measured voltage U_{measured} and steady state voltage

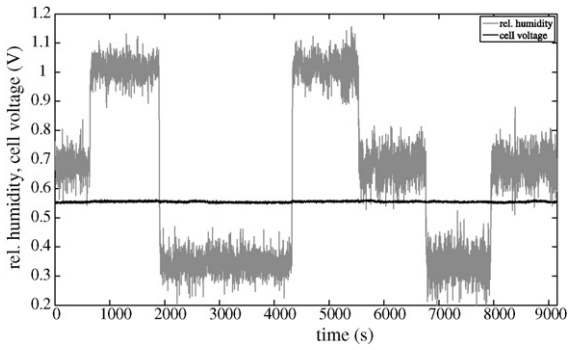

Fig. 7. Variation of humidity and measured step response of voltage in case of an operating point with low dynamic (i = 0.9 A cm^{-2}, λ_c = 3, λ_a = 3, p_c = 1.5 bar, p_a = 1.5 bar, rh$_a$ = 0.33, T = 70 °C, T = 10 K, c_{H_2} = 1).

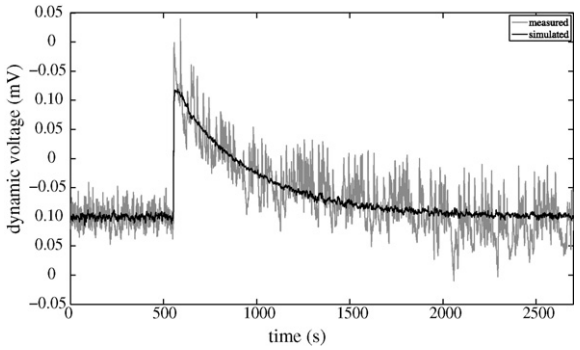

Fig. 8. Comparison of measured dynamic voltage and dynamic voltage, simulated by a transfer function with $T_D = 633.9$ and $K_D = -22.2$ ($i = 1.4\,A\,cm^{-2}$, $\lambda_c = 3.5$, $\lambda_a = 1.5$, $p_c = 2.1$ bar, $p_a = 1.7$ bar, $rh_a = 33\%$, $T = 70\,^{\circ}C$, $T = 0$ K, $c_{H_2} = 1$, $rh_{c,1} = 1.00$, $rh_{c,2} = 0.33$).

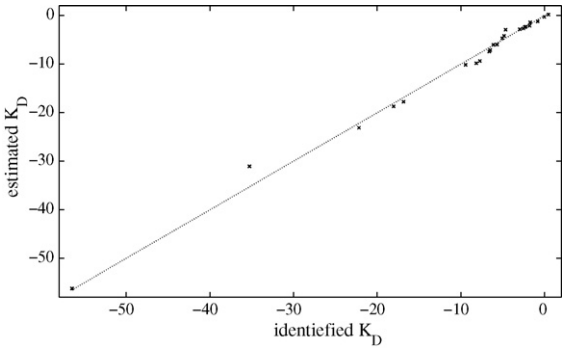

Fig. 9. Identified vs. estimated K_D using Eq. (7) ($\times$ = fitted K_D, dotted line = ideal regression).

U_{static} (Eq. (17)), was identified for every run and analysed in view of describing its behaviour:

$$U_{dynamic} = U_{measured} - U_{static} \tag{17}$$

The dynamic voltage shows in all cases the typical behaviour of a 1st-order proportional-differential transfer function PDT_1 which is described by the following equation:

$$G(s) = \frac{K_D s}{T_D s + 1} \tag{18}$$

The dynamic voltage was simulated by using this transfer function. In this respect, K_D is characterising the height of the step response and T_D the time delay till the steady state is reached again. One of these simulated step responses in comparison to the measured dynamic behaviours is shown in Fig. 8.

The simulated step in cathode gas humidity by an identified PDT_1 transfer function fits very well the measured dynamic voltage and was therefore a promising way to characterize the fuel cell.

5.1. Linear modelling

First, a simple linear dynamic model is investigated. To describe the dynamic cell voltage, the previously introduced PDT_1 transfer function (Eq. (18)) with constant coefficients K_D and T_D is used. The 174 steps for parameter estimation can be fitted best with a $K_D = -9.1$ and a $T_D = 633.9$.

5.2. Nonlinear modelling

The experimental analysis of all 174 steps individually, a strong correlation between K_D and T_D can be observed. Due to this high correlation, the delay time is fixed to the value of the linear model as $T_D = 633.9$. The estimated values for K_D vary in a range from 0 to −60. However, the step height K_D depends nonlinear on the input variables. To develop a precise and simple polynomial, witch describes the dependency of K_D regarding the operating conditions, a stepwise multiple-regression analysis is used.

In the first step, the matrix X is set up. In the first column, ones are placed to include a constant term in the polynomial. Columns 2–10 are filled with the untransformed inputs, as they are i, λ_c, λ_a, p_c, p_a, rh_a, T_{in}, ΔT, and c_{H_2}. Columns 11–19, with the logarithm of the inputs, columns 20–28, with the exponential transformation, in columns 29–37, the reciprocal inputs, and columns 38–46, the square root of the 9 inputs. Secondly, the matrix X is expanded in the columns 47–1036 with all two-way-interactions of columns 2–46 like $i\lambda_c$, $i\lambda_a$, ip_c, etc. Finally, columns 1037–1081 are added with the quadratic values of columns 2–46 to gain a full quadratic polynomial.

In the second step, the stepwise multiple-regression analysis is initialized considering ξ_{1-46} to be nonzero and therefore be included terms in the polynomial. All other coefficients $\xi_{47-1081}$ are initialized to be zero and therefore off the polynomial. The remove threshold Ψ_{out} is set to $\Psi_{out} = 0.05$ and the enter threshold Ψ_{in} is set to $\Psi_{out} = 0.1$.

Thirdly, stepwise multiple-regression is started. The probability of the null hypothesis Ψ_θ of all coefficients ξ_θ is calculated as described in chapter 2 using Eqs. (5)–(12). After that, all non-significant terms are removed and significant terms which have been previously off are included to the polynomial.

Finally, the third step is repeated 12 times while no change in individual term significance can be observed.

The result of the stepwise multiple-regression analysis, using the untransformed 9 inputs and the proposed transformation, are 12 significant terms as they are summarized in Table 2.

The R^2_{adj} of the stepwise multiple-regression is quite good with $R^2_{adj} = 0.9849$ which can be visualized with a estimated K_D (calculated with the model shown in Table 2) vs. identified K_D (identified with the measured data) plot as drawn in Fig. 9 where every cross represents a different data set in an own operation point of the PEMFC system.

6. Model validation

Always if experimental based system identification methods are used, the developed models must be validated, using independent experiments. From the 606 experimental step data sets, just 174 have been used during parameter estimation process. To do the validation of the postulated polynomial to calculate K_D as a function of PEMFC operation conditions, the 432 not jet used experimental data sets are used.

Table 2
Result of stepwise multiple-regression analysis of PEMFC operating conditions influence at K_D

No.	θ	ξ_θ	Term $X(\theta)$	Ψ_θ
1	1	9.754E+01	1	0.000E+00
2	2	−7.033E+01	I	7.276E−06
3	3	−4.098E+00	λ_c	9.494E−07
4	5	3.030E+00	p_c	1.537E−02
5	8	1.496E−01	T_{in}	4.005E−02
6	9	−4.791E+00	ΔT	3.887E−06
7	335	1.415E+00	$\Delta T \exp(i)$	9.448E−08
8	355	−3.189E+00	$\Delta T/\lambda_a$	2.474E−06
9	577	−1.035E+00	$\exp(rh_a)\log(\lambda_a)$	5.107E−03
10	649	−3.484E−08	$\Delta T/c_{H_2}$	5.429E−18
11	700	1.838E+03	$\log(i)/T_{in}$	4.285E−03
12	906	−1.315E+02	$1/(\lambda_c\,\Delta T)$	2.705E−14

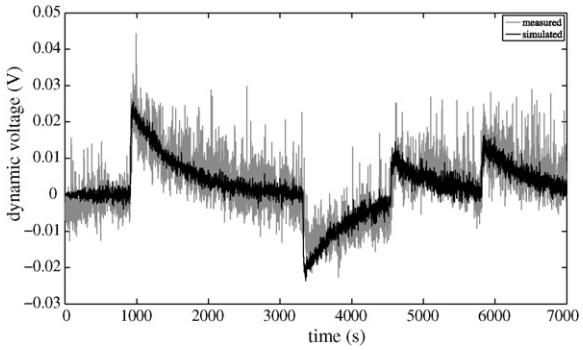

Fig. 10. Comparison of measured and simulated dynamic voltage of a run with low dynamic voltage ($i = 1\,\mathrm{A\,cm^{-2}}$, $\lambda_c = 1.9$, $\lambda_a = 1.4$, $p_c = 1.4$ bar, $p_a = 1.6$ bar, $\mathrm{rh_a} = 0.50$, $T = 55\,^{\circ}\mathrm{C}$, $T = 10\,\mathrm{K}$, $c_{\mathrm{H_2}} = 1$).

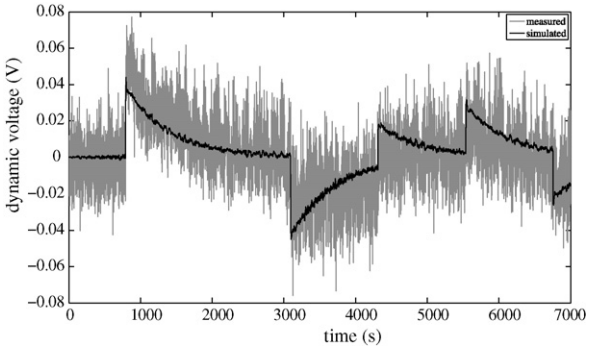

Fig. 11. Comparison of measured and simulated dynamic voltage of a run with high dynamic voltage ($i = 0.9\,\mathrm{A\,cm^{-2}}$, $\lambda_c = 1.4$, $\lambda_a = 1.4$, $p_c = 1.8$ bar, $p_a = 1.8$ bar, $\mathrm{rh_a} = 0.66$, $T = 55\,^{\circ}\mathrm{C}$, $\Delta T = 10\,\mathrm{K}$, $c_{\mathrm{H_2}} = 1$).

A calculated degrees of freedom adjusted R-square for the validation data of $R^2_{\mathrm{adj}} = 0.9689$ indicates a good generalization of the developed polynomial. The match between measured and calculated dynamic voltage using K_D from the polynomial in Eq. (18) for two representative runs is given in Figs. 10 and 11. In contrast to Figs. 6 and 7 shows a pure dynamic of the mean cell voltage in different operation points. Fig. 10 has a lower dynamic with about 45 mVpp (mV peak to peak) in comparison to Fig. 11 with a higher dynamic with about 80 mVpp.

It is obviously, that the introduced method, the combination of transfer function and nonlinear regression of K_D, describes the dynamic voltage very satisfying. Especially, the fact that different dynamic behaviours, the second run curve has a dynamic voltage twice as big as the first one, were simulated correctly only by knowing the operating conditions is a success.

Particularly the comparison of the pure static, the linear dynamic, and the nonlinear dynamic model give a good impression of the realized improvement in PEMFC modelling. For comparing these three models and thus evaluate our new method, the error between calculated dynamical voltage and simulated one is analysed statistically. The residual histograms in Figs. 12–14 are similar to the Gaussian Distribution and the shape of the Distribution delivers an estimation of the simulation quality. The first plot (Fig. 12), is performed without a consideration of the dynamic behaviour and is therefore a good reference for the dynamic simulations of stack voltage.

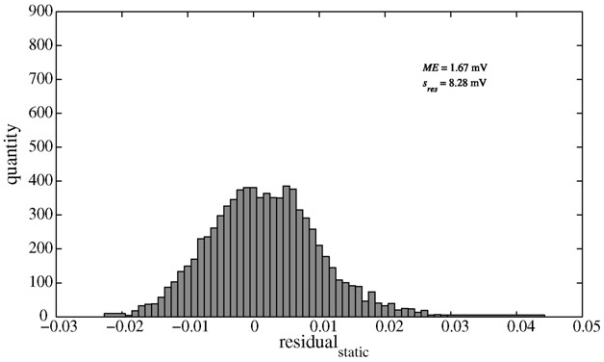

Fig. 12. Residual histogram of the static model.

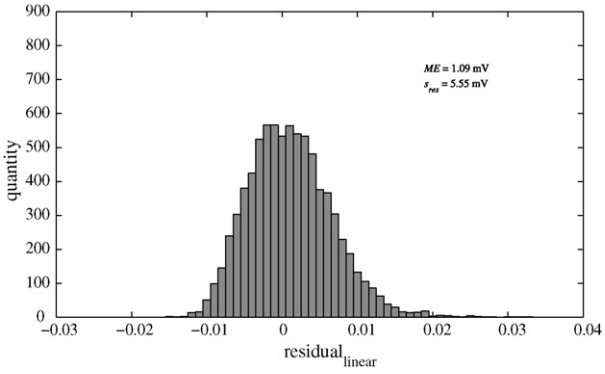

Fig. 13. Residual histogram of the linear model.

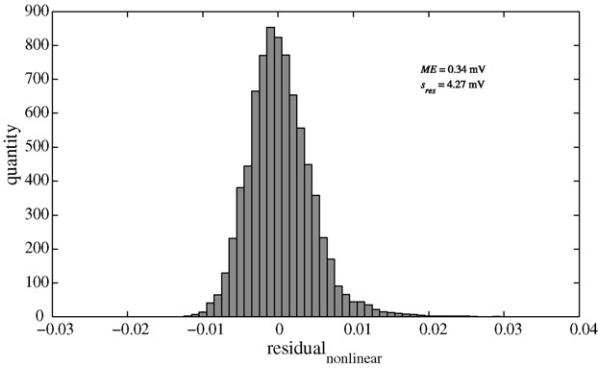

Fig. 14. Residual histogram of the nonlinear model.

Figs. 13 and 14 show the mean error ME could be minimized at about 35% by using a $\mathrm{PDT_1}$-element with a constant K_D and a further significant improvement of about 69% is achieved by replacing this

Table 3
Results of model validation

Model	ME (mV)	$1 - \frac{\mathrm{ME}}{\mathrm{ME_{static}}}$ (%)	s_{res} (mV)	$1 - \frac{s_{\mathrm{res}}}{s_{\mathrm{res,static}}}$ (%)	R^2_{adj}	$1 - \frac{1-R^2_{\mathrm{adj}}}{1-R^2_{\mathrm{adj,static}}}$ (%)
Static	1.67	0.0	8.28	0.0	0.8943	0
Linear	1.09	34.7	5.55	33.0	0.9353	38.8
Nonlinear	0.34	79.6	4.27	48.4	0.9689	70.6

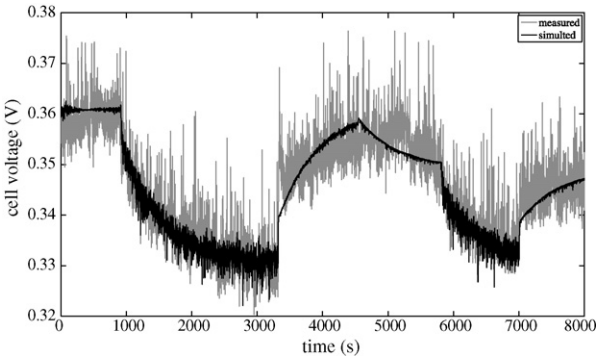

Fig. 15. Comparison of simulated and measured mean stack voltage of the nonlinear model ($i = 1\,A\,cm^{-2}$, $\lambda_c = 1.9$, $\lambda_a = 1.4$, $p_c = 1.4$ bar, $p_a = 1.6$ bar, $rh_a = 0.50$, $T = 55\,^{\circ}C$, $\Delta T = 10$ K, $c_{H_2} = 1$).

constant K_D by using the polynomial given in Table 2. Compared, the pure static model a total reduction of mean error of 80% can be realized. A final mean error of nearly zero (ME = 0.34 mV) proves, how accurate the dynamic voltage can be simulated. The reduction of standard error from 8.28 to 4.27 mV, if the nonlinear model is added to the static model, equals nearly a bisection of the error.

In Table 3, the results of the model validation are summarized. Nearly 90% of overall precision is related to the stationary model as the $R^2_{adj,static}$ value indicates. 38.8% of gas humidity-related voltage dynamics can be described with a simple PDT_1 transfer function using constant coefficients. A highly precise nonlinear model is developed, which reduces model errors by 70.6%. Such a model is able to fulfill highest demands for system simulation and power train optimization purposes.

In Fig. 15, the mean cell voltage of the investigated PEMFC stack is plotted for a complete cathode humidity cycle. The good performance, indicated by the residual histogram, can be visualized. The noise of the simulated voltage is related the noise of the measured 9 inputs, which are fed directly into the model. If stable inputs are used, the simulated voltage is smooth.

7. Summary and outlook

A general method for simulating the gas humidity-related voltage dynamics of a PEMFC stack is developed and introduced. For this purpose, a new humidification system has been developed and validated against highly precise CMDPHs. The DSI allows dynamic investigations of a PEMFC without the need of humidity measurements and is able to provide experimental data to identify a dynamic model. Step responses of the mean cell voltage, after varying the humidification of the cathode, are measured and the resulting behaviour is well described by a PDT1-element. The proportional constants K_D, gained from parameter estimation, are used in combination with the operating conditions to identify a 2nd-order polynomial by a stepwise multiple-regression analysis, which approximates accurately the dynamical behaviour of all steps. Transfer function and regression equation are successfully validated. The fit between simulated and experimental data is high and thus a novel dynamic model for the stack voltage is successfully introduced.

Possible applications of this new method are, for example, the substitution of experiments by simulations, and the development of an operating strategy of PEMFC powered drive trains.

Further work should be done, by investigate more operating conditions to improve the valid range of the model.

Acknowledgements

We would like to thank our colleagues at the Department of Measurement, Control and Microtechnology, University of Ulm and Daimler AG, shearing their great knowledge with us, for their helping hands with the experimental setup, and the fruitful discussions.

References

[1] R. O'Hayre, S.W. Cha, W. Colella, F.B. Prinz, Fuel Cell Fundamentals, John Wiley & Sons, Hoboken, 2006.
[2] J. Larminie, A. Dicks, Fuel Cell Systems Explained, John Wiley & Sons, West Sussex, 2003.
[3] M. Meiler, O. Schmid, M. Schudy, E.P. Hofer, J. Power Sources 176 (2007) 523–528.
[4] T.E. Springer, T.A. Zawodzinski, S. Gottesfeld, J. Electrochem. Soc. 138 (1991) 2234–2242.
[5] H. Görgun, M. Arcak, F. Barbir, J. Power Sources 157 (2005) 389–394.
[6] O.A. Alduchov, R.E. Eskridge, J. Appl. Meteorol. (1995) 601–609.
[7] D. Urban, J. Mayerl, Regressionsanalyse: Theorie, Technik und Anwendung, 2. Aufl. Wiesbaden VS-Verlag, 2006.
[8] S. Rässler, P. Mertens, Prognoserechnung. 6. Aufl. Physica Verlag, 2005.
[9] R. Isermann, Identifikation dynamischer Systeme, Springer Verlag, Berlin, 1988.
[10] U. Graf, H.-J. Henning, K. Stange, P.T. Wilrich, Formeln und Tabellen der angewandten mathematischen Statistik, Springer Verlag, Berlin, 2007.
[11] L. Fahrmier, R. Künstler, I. Pigeot, G. Tutz, Statistik: Der Weg zur Datenanalyse 6. Aufl., Springer Verlag, Berlin/Heidelberg, 2007.
[12] K.R. Koch, Parameterschätzung und Hypthesentests in linearen Modellen. 3. Aufl. Dümmler, Verlag, Bonn, 1997.
[13] U. Kiencke, R. Eger, Messtechnik, 6. bearb. Aufl., Verlag, Springer, Berlin, 2008.
[14] D.W. Spitzer, W. Boyes, Copperhill Pointer (2003).
[15] H. Sun, G. Zhang, L.J. Guo, S. Dehua, H. Liu, J. Power Sources 168 (2007) 400–407.
[16] W. Friede, IEEE Trans. Power Electron. 19 (September (5)) (2004).
[17] C. Song, C.J. Chua, et al., J. Hydrogen Energy 33 (2008).
[18] H. Nishikawa, R. Kurihara, J. Power Sources 155 (2005).